Proceedings of DETC'03
ASME 2003 Design Engineering Technical Conferences and Computers and Information in Engineering Conference
Chicago, Illinois, USA, September 2-6, 2003

DETC2003-48053

ANALYSIS OF THE MESH CHARACTERISTICS OF HYPOID GEAR PAIR DYNAMICS

Hongbin Wang
Eaton Corporation, Innovation Center
26201 Northwestern Highway, Southfield, MI 48076

Teik C. Lim
University of Cincinnati
Mechanical, Industrial and Nuclear Engineering
P.O. Box 210072, Cincinnati, OH 45221

ABSTRACT

Most of the current models employed in analyzing the dynamics of hypoid or bevel gear pair systems are based on approximate representations of the tooth meshing kinematics. The approximate gear mesh representations that account for tooth contact position and load line of action vector are normally derived from experimental observations or semi-empirical considerations. Moreover, the resultant dynamic model is often linear with time-invariant coefficients. The fundamental behavior of the time-varying mesh points and load line of action vectors, which can be important characteristics of the hypoid gear pair system, have not been fully explored. To address this issue more in-depth, the current study examines the inherent spatial and time-varying tooth meshing positions and normal load vectors of typical hypoid gear pairs applied in automotive systems. Numerical results of the quasi-static gear tooth contact analysis using 3-dimensional finite element models are compared to the theoretical data produced by a set of analytical tooth contact analysis equations based strictly on gear geometry formulation. The potential effects of gear meshing characteristics on dynamic transmission error as well as torsional vibration response are also discussed.

INTRODUCTION

With increased requirements for higher speeds, heavier loads, and lighter weights in gear design, the prediction and control of dynamic mesh forces and resulting vibration transmissibility have become more important. This is because the fundamental dynamic behaviors of the gears are believed to have direct control on durability, vibration, and acoustic noise response. In fact, the problem may be more acute in hypoid gear set, which is widely used in rear axle drive applications to transmit rotational motion between two perpendicular, non-intersecting axes. Due to unique shafting configuration, the directed line segment of the dynamic mesh force generated is oriented at an oblique angle relative to the input and output rotational axes. This unique characteristic tends to worsen the dynamic problem compared to other parallel axis gearing applications.

Unlike parallel axis gears, not much effort has been devoted to investigate the dynamics of hypoid gears. This is because of its inherently more complex geometry, mesh pattern, and dynamic coupling between torsional and translational vibration. Most of the earliest set of research investigations on hypoid gears mainly focus on (i) the synthesis of machine tool and cutter settings to manufacture higher precision tooth profiles in order to achieve the desired transmission error and contact patterns (Kawasaki et al. [1], Donno, Litvin [2], Feng, Litivn [3], and Litivn [4-5]); (ii) stress and load distributions that are partly applied to determine the loaded transmission error (Krenzer [6], Gosselin, Cloutier, Nguyen [7], Mark [8], Vijayakar [9]); and (iii) purely torsional dynamic simulations based on semi-empirical mesh point and force vector representations that are essentially time-invariant (Kiyono, Fujii, Suzuki [10], Rautert, Kollmann [11], Donley, Lim, Steyer [12]). None of the dynamic simulation work satisfactorily addresses the time-varying mesh point and force vector characteristics, which are predominant in hypoid gearing.

One of the more comprehensive works to investigate the vibration characteristics of hypoid gear set was conducted by Cheng and Lim [13-15]. The torsional and translation couplings are also considered in their modeling. A 14 degrees-of-freedom (DOF) linear time invariant (LTI) model was proposed for a generic driver-gear-load system. Modal

properties and force transmissibility were studied, and critical modes were identified. Numerous simulations were performed to investigate the effects of various gear parameters including pinion offset, spiral angle, etc. Furthermore, a 10-DOF non-linear time-varying (NLTV) model was also developed that ignores the bending rotation coordinates of the pinion and gear. The nonlinearity elements considered include backlash and mesh stiffness. This proposed model provided the first glimpse of nonlinear behavior in lightly loaded hypoid gear pair. No other studies found in the open literature that is as comprehensive and complete as these analyses. However, the models proposed by Cheng and Lim basically still assume time-invariant mesh point and force vector, which are not exactly valid.

In this paper, the fundamental nature of the hypoid gear meshing action, in which the mean contact position vector and line of action vary with time, is examined from the viewpoint of formulating a dynamic model. Obviously, the resultant motions of the hypoid gear elements must be described in a 3-dimensional coordinate space rather than in plane form typically used for spur gears. The results presented here will be used to construct a suitable gear mesh characteristic for use in subsequent non-linear time-varying vibration response simulation. The mesh results obtained from models that assume either single-point or multi-point coupling gear mesh representation will be compared. The central discussions will be on the variations of the pitch point and line of action vector.

SINGLE-POINT COUPLING MESH MODEL

The simplest lumped parameter gear mesh model that assumes a single-point coupling mesh representation, as shown in Figure 1, is commonly used in the simulation of gear dynamics. The two mating gears with mass moment of inertia I_i and base radius R_i (subscript i equals to 1 for the driver gear or 2 for the driven gear) are coupled by a linear, unidirectional, infinitesimal spring-damper element with stiffness K_m and damping C_m. The spring is located at a certain radius from the center of the gear (generally known as pitch radius for spur/helical gears), and acts along the mesh line of action. Both the line of action vector and the meshing point are frequently assumed to be time-invariant, especially in spur and helical gear cases. The system is excited by a periodic transmission error e(t). This model is designed primarily to represent the mean gear mesh behavior, whose mesh stiffness is given as a function of tooth flexibility and other types of gear compliance.

Even though the single-point coupling gear mesh model is simple and widely used, it is inadequate for analyzing problems in hypoid gear dynamics. Firstly, the variations of the meshing point and the line of action vector are not considered. Secondly, the dynamic interaction between consecutive gear mesh interfaces, especially since hypoid gear pairs possess relatively high contact ratios, is not evaluated. Thirdly, the application of the single-point coupling mesh model is mainly suitable for spur and helical gears where the gear mesh forces normal to the tooth surface always act in the same line of action direction. Therefore, using only a single equivalent mesh stiffness to represent the tooth engagement process may be sufficient for these parallel axis gears. This is not the case in hypoid gears. For hypoid gear, a higher order mesh model is actually needed to capture the more complex gear engagement process where the meshing points and line of action vectors exhibit significant time and spatial-varying behavior. This is due to the fact that the mating pinion and gear teeth roll and slide along their pitch surfaces as they pass through the engagement zone. Also, there is more than one pair of teeth in contact at any given time with each tooth pair having quite different line of action vectors. To account for these distinctive meshing behaviors, a multi-point coupling mesh model is proposed as described next.

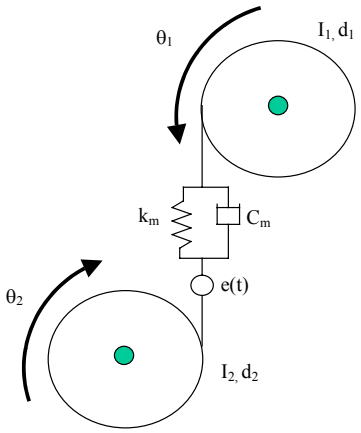

Figure 1. A single-point coupling mesh model.

MULTI-POINT COUPLING MESH MODEL

The concept of multi-point coupling mesh model is shown in Figure 2. The fundamental concept is based on the assumption that more than one tooth mesh coupling interface may exist at any given time. The number of mesh interfaces is dependent on contact ratio, load and gear rotation position. Each mesh interface is represented by a set of meshing point, line of action and mesh stiffness. Both backlash and Coulomb friction non-linearity can be incorporated in each mesh interface as well. Due to the fact that the mesh point paths and line of action vectors for the tooth mesh interfaces are not collinear, this new mesh model can more accurately reflect the true nature of the gear engagement process compared to the single-point coupling concept. The use of this proposed concept should be able to predict the system response more accurately and provide new results that are not possible in the past. Also, the effects of time-varying characteristics of mesh

can be included in the dynamic analysis with fewer assumptions needed, the limitation of low contact ratio assumed in the previous single-point coupling mesh model can be removed.

In order to construct such as proposed multi-point coupling mesh representation, detailed meshing pattern from a 3-dimensional gear tooth contact analysis is required. This information can be derived from the Contact Analysis Program Package (CAPP) developed by Vijayakar [16]. Using CAPP, a set of quasi-static analysis is performed to obtain the meshing results at each discrete gear angular position. The meshing patterns are condensed further to give a mean mesh point and a resultant line of action in which the dynamic mesh force vector is assumed to act along. Unlike all other previous gear mesh models that are based on either empirical design equation or pure geometry formulation, this proposed analysis yield the true mesh representation under load.

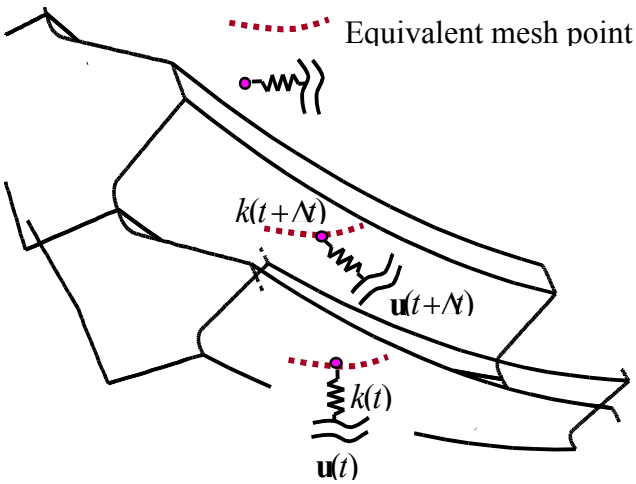

Figure 2. Multi-point coupling gear mesh model.

The new multi-point coupling gear mesh model also serves as a direct link between the static gear tooth contact analysis and gear pair system dynamics. In our analysis, the predicted contact information from CAPP is further processed to obtain the relevant gear mesh parameters. The gear mesh model can then be implemented in the dynamic model without having to make further assumptions except those used in the quasi-static tooth contact analysis. Furthermore, the proposed multi-point coupling gear mesh model has the potential to be easily applied in system level vibration problem where most of the components are modeled using the finite element method (FEM).

GEAR MESH ANALYSIS

From the detailed quasi-static tooth contact analysis, the mesh areas on the tooth surfaces are discretized into a series of smaller cells. Each cell contains a localized compliance c_{ij} that is a function of the spatial dimensions, gear mesh position, and applied mean torque. The position vector of the contact cell n in the coordinate system S(l) (l=1,2 for pinion, and gear, respectively, and l=0 for a fixed coordinate system with the origin at the crossing point of pinion and gear rotation axis when viewed from above) is $\mathbf{r}_{nj}^{(l)} = \{x_{n1j}^{(l)}\ x_{n2j}^{(l)}\ x_{n3j}^{(l)}\}^T$, and the unit normal vector is given by $\mathbf{n}_{nj}^{(l)} = \{n_{n1j}^{(l)}, n_{n2j}^{(l)}, n_{n3j}^{(l)}\}^T$, as shown in Figure 3.

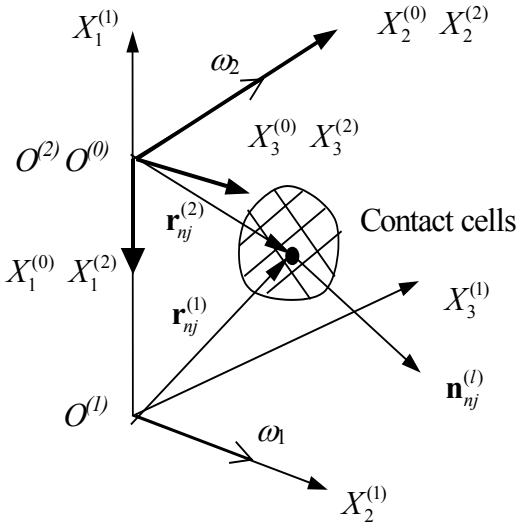

Figure 3. Determination of resultant forces and moments using the contact cell concept.

The projection of the unit normal vector into the tangential direction of rotational motion relative to the S(l) coordinate system represented by i axes can be expressed as

$$\lambda_{n1j}^{(l)} = \mathbf{n}_{nj}^{(l)} \cdot (\mathbf{i}^{(l)} \times \mathbf{r}_{nj}^{(l)}) = n_{n3j}^{(l)} x_{n2j}^{(l)} - n_{n2j}^{(l)} x_{n3j}^{(l)}. \quad (1)$$

$$\lambda_{n2j}^{(l)} = \mathbf{n}_{nj}^{(l)} \cdot (\mathbf{j}^{(l)} \times \mathbf{r}_{nj}^{(l)}) = n_{n1j}^{(l)} x_{n3j}^{(l)} - n_{n3j}^{(l)} x_{n1j}^{(l)}. \quad (2)$$

$$\lambda_{n3j}^{(l)} = \mathbf{n}_{nj}^{(l)} \cdot (\mathbf{k}^{(l)} \times \mathbf{r}_{nj}^{(l)}) = n_{n2j}^{(l)} x_{n1j}^{(l)} - n_{n1j}^{(l)} x_{n2j}^{(l)}. \quad (3)$$

where $\mathbf{i}^{(l)}$, $\mathbf{j}^{(l)}$ and $\mathbf{k}^{(l)}$ are the triad of unit vectors that define the coordinate system S(l). Consider the resultant normal force $F_{\delta ij}^{(l)}(t)$ and friction force $F_{\tau ij}^{(l)}(t)$ acting on gear member l along the i-axis, where i=1,2 and 3, corresponding to a specific pair of teeth in contact (denoted by j) at any given time t,

$$F_{\delta ij}^{(l)}(t) = \sum_{n=1}^{n_j} n_{nij}^{(l)} k_j^{(l)}(n) \delta_j^{(l)}(n) = \mathbf{N}_j^{(l)}(t) [C_{\vartheta}^{(l)}(t)]^{-1} \Delta_{\vartheta}^{(l)}(t) = n_{ij}(t) W_j(t), \quad (4a)$$

$$F_{\tau ij}^{(l)}(t) = \sum_{n=1}^{n_j} \mu s_{nij}^{(l)} k_j^{(l)}(n) \delta_j^{(l)}(n) = \mu \mathbf{V}_j^{(l)}(t) \left[C_{\vartheta}^{(l)}(t)\right]^{-1} \Delta_{\vartheta}^{(l)}(t) = \mu \tau_{ij}(t) W_j(t). \quad (4b)$$

Here, n_j is the total number of contact cells found on tooth pair j, $\delta_j^{(l)}(n)$ is the deformation of cell n, and $n_{nij}^{(l)}$ and $v_{nij}^{(l)}$ are the directional components along the i-axis of the normal and friction forces for cell n of gear member (l). The above equations essentially give the average normal and frictional loads by summing the forces on the individual cells. Since $W_j(t)$ is the equivalent normal force vector for mesh interface j, and $n_{ij}(t)$ and $\tau_{ij}(t)$ are directional components along the i-axis of the normal and frictional forces. Their elements make up the corresponding directional vectors $\mathbf{n}_j$ and $\boldsymbol{\tau}_j$. It should be noted that both vectors are functions of mesh position and applied pinion torque.

The resultant moments of each contact cell's normal and friction forces about the i-axis in mesh interface j are calculated from:

$$M_{\delta ij}^{(l)}(t) = \sum_{n=1}^{n_j} \lambda_{nij}^{(l)} k_j^{(l)}(n) \delta_j^{(l)}(n), \tag{5a}$$

$$M_{\tau ij}^{(l)}(t) = \sum_{n=1}^{n_j} \mu \tau_{nij}^{(l)} k_j^{(l)}(n) \delta_j^{(l)}(n). \tag{5b}$$

The position of the mesh point on gear member (l) relative to the gear centroid at the interface j is $\mathbf{r}_{mj}^{(l)}(t) = \left\{ x_{m1j}^{(l)} \quad x_{m2j}^{(l)} \quad x_{m3j}^{(l)} \right\}^T$, and is found by averaging the pressure weighted contact location of the cells. The mesh points are not necessarily the geometric center of the meshing cells since both the force and gear ratio continuity must be maintained in the process. It is explicitly given by

$$\mathbf{r}_m^{(l)} = \frac{\sum_{n=1}^{n_j} \mathbf{r}_{nij}^{(l)} k_j^{(l)}(n) \delta_j^{(l)}(n)}{\sum_{n=1}^{n_j} k_j^{(l)}(n) \delta_j^{(l)}(n)}. \tag{6}$$

The mesh stiffness of each interface is calculated by fixing the gear and rotating the pinion about the nominal operational axis. Thus, the loaded transmission error along the line of action direction for interface j is

$$\delta_{Lj} = \mathbf{u}^{(1)} \bullet \mathbf{n}_j = \boldsymbol{\theta}^{(1)} \times \mathbf{r}_j^{(1)} \bullet \mathbf{n}_j = \theta_L (n_{1j} x_{m3j}^{(1)} - n_{3j} x_{m1j}^{(1)}). \tag{7}$$

Assuming that the mesh points for loaded and unloaded conditions are identical, the normal mesh stiffness $k_j(t)$ for the mesh interface j can be shown to be

$$k_j(t) = \frac{W_j(t)}{\delta_{Lj} - \delta_{0j}} = \frac{W_j(t)}{(\theta_L - \theta_0)(n_{1j} x_{m3j}^{(1)} - n_{3j} x_{m1j}^{(1)})}. \tag{8}$$

where θ_L and θ_0 are the angular transmission errors under loaded and unloaded conditions, respectively, and $W_j(t)$ is the equivalent normal mesh force at the mesh interface j. Also, note that the instantaneous $k_j(t)$ is a function of load, tooth geometry, and angular position. Thus, the mesh properties obtained through these procedures are time-varying and load-dependent. The procedures to compute the mesh stiffness, line of action vector and friction force vector for a particular mesh interface are summarized in Figure 4.

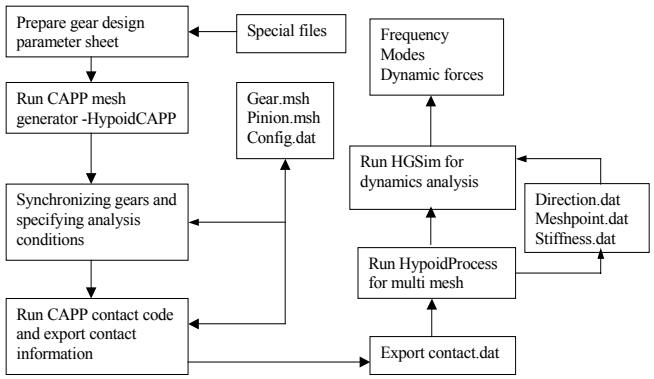

Figure 4. Summary of multi-point coupling gear mesh analysis.

SIMULATION RESULTS

First, a light load case is studied to allow the comparison of the results of the proposed multi-point coupling gear mesh theory to an existing mesh representation based purely on geometric data only where no load is considered. In this case, the quasi tooth contact analysis applying CAPP is performed by imposing a small nominal force in order to keep the teeth in contact. In this paper, the torque used is about 5 Nm, which is small relative to the normal working torque of several thousands Nm. The use of this small load is to ensure that the quasi-static tooth contact analysis result is dictated mainly by the tooth geometry parameters only.

The directional cosine angles of the line of action vector from the geometry-based single-point coupling mesh model and those from the newly calculated CAPP-based multi-point coupling mesh model are compared in Figure 5(a-c) for the x, y, and z axis, respectively. From these curves, it can be seen that under very light load, only one pair of teeth has significant contact. Furthermore, fairly good agreements are observed between the two different models. The comparison of the coordinates of the meshing points is shown in Figure 6 (a-c) for the x, y, and z coordinates, respectively. Again from these curves, it can be seen that the mesh points computed from both methods possess the same general trend.

The mesh information obtained from the present method is further used to calculate the mean mesh data as shown in Table 1. Here, the mesh information from the single-point coupling gear mesh model is also listed for comparison to the spatially averaged mesh information from the proposed multi-point coupling gear mesh model. In general, as expected, we see fairly good agreement between these two models. It may be noted that the correct gear ratio is also maintained in the data reduction process.

Table 1. Comparisons of the predicted mesh point coordinates and line of action vector.

Mesh Model	x_f (mm)	y_f (mm)	z_f (mm)	n_{xf}	n_{yf}	n_{zf}	Gear ratio
Geometry-based	-41.96	138.18	1.23	-0.1835	-0.7578	-0.6257	4.302
CAPP-based	-41.57	138.53	0.568	-0.1818	-0.7520	-0.6326	4.294

In the case of a higher torque load, the results are shown in Figure 7. Here, the directional cosine angles of the line of action vectors for both light and high load cases are compared. Both sets of results are computed by again applying the proposed CAPP-based multi-point coupling gear mesh model. It may be noted that the differences as large as 4 degrees are observed, which may produce significant differences in system response. Figure 8 shows the comparisons of the coordinates of meshing points for light and higher load results. The mesh points are observed to be quite different between the two cases. The mesh point location along the gear rotation axis appears to be most influenced by the load level applied. This is because under load, the mesh point will shift along the width of the tooth surface. From these plots, it can be concluded that the load conditions strongly influence the meshing properties of the gear sets. This suggests that the single-point coupling gear mesh model, which is generally based on geometry relations, is inferior under heavier load.

Another important aspect of gear mesh properties is the definition of the mesh stiffness. Previous representation typically uses simple beam bending equation or measured data. The mesh stiffness is assumed either to be time-invariant or simple square-wave function. Hence, it is very difficult to find a more exact mesh stiffness representation as a function mesh location and load level without adopting many assumptions. Using the proposed multi-point coupling gear mesh concept, this difficulty can be overcome as the mesh stiffness is defined for each meshing interface as a function of angular position. Figure 9 shows a set of curves showing the variation of mesh stiffness over one mesh cycle. The time-invariant mesh stiffness model used previously is also shown in the form of a straight horizontal line for comparison. From this comparison, the previous time-invariant model clearly cannot be used to simulate the true engagement process.

CONCLUDING REMARKS

A new gear mesh model for hypoid gears has been proposed, which can be applied to formulate the right-angle geared rotor dynamic model. The new gear mesh model yields a multi-point coupling gear mesh representation by applying the results of the quasi-static tooth contact analysis. The proposed gear mesh model is capable of representing the time and spatial-varying mesh properties of the hypoid gear pair under loaded condition more precisely. Comparison of the results of the proposed gear mesh model with the current geometry-based gear mesh theory for no load case shows excellent agreement. Furthermore, a more direct connection between the results of the gear quasi-static tooth contact analysis and gear dynamics is made possible using this proposed gear mesh model. This connection, which has not been derived prior to this research work, can be applied to gain a better understanding of the gear mesh properties and the possible influences on system dynamics.

ACKNOWLEDGEMENTS

This material is based upon work partly supported by the National Science Foundation under Grant No. 9978581, and the Hypoid/bevel Gear Dynamic Modeling Consortium under the direction of Prof. Teik C. Lim. Also, the permission granted by Dr. Sandeep Vijayakar of ANSOL to use CAPP for part of the calculations is greatly appreciated.

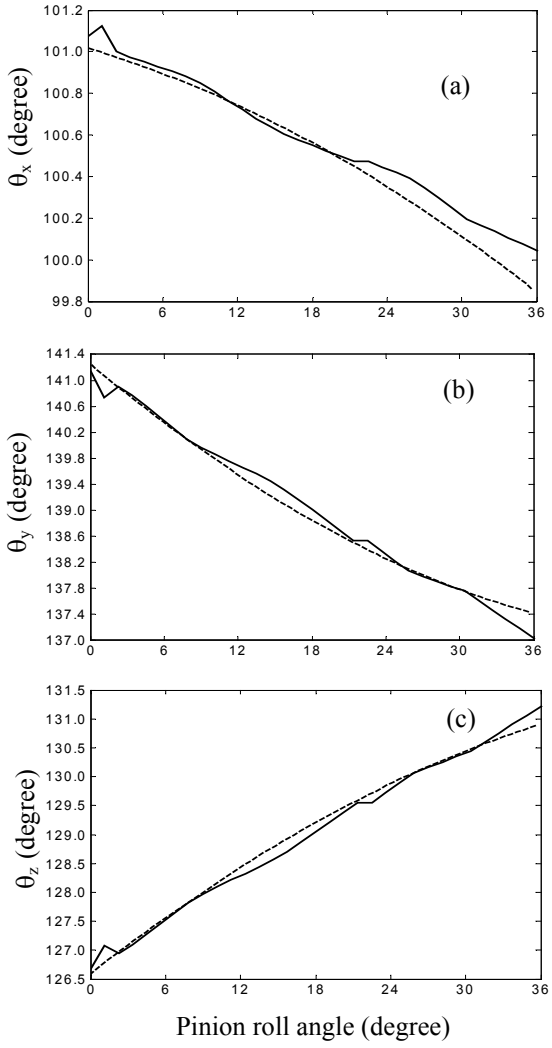

Figure 5. Comparison of the directional cosine angles relative to the (a) x-axis, (b) y-axis, and (c) z-axis. (Keys: ——, CAPP-based ; ·····, geometry-based)

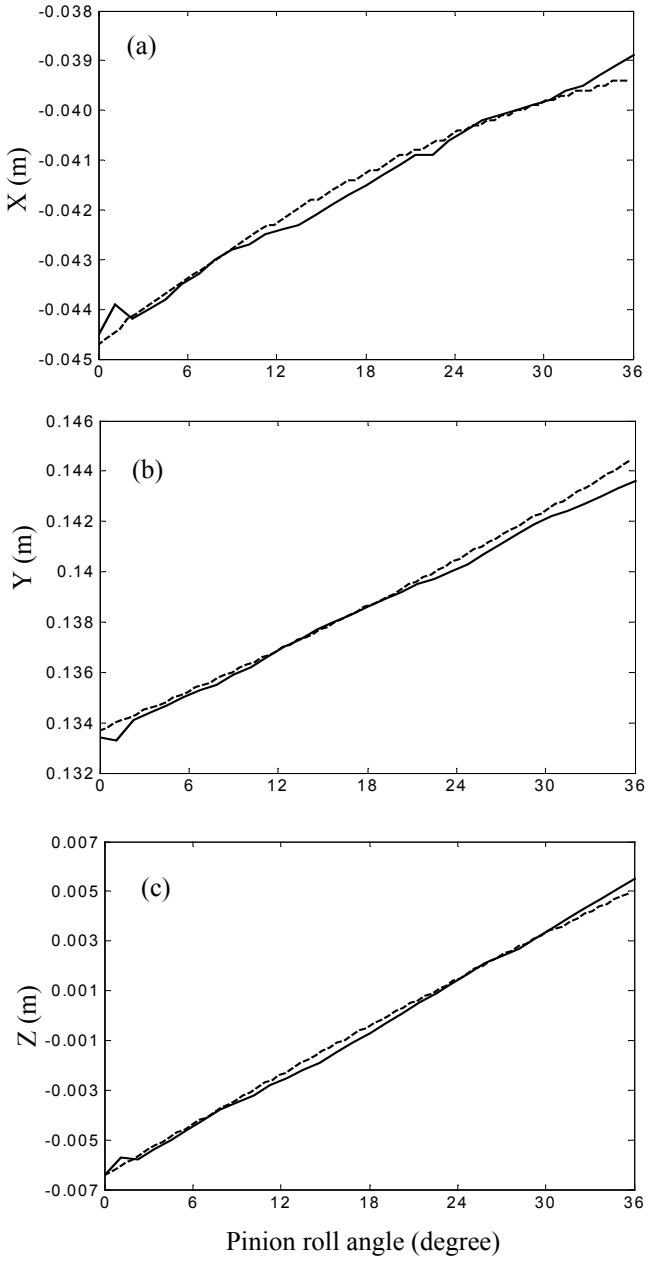

Figure 6. Comparison of the mesh point positions: (a) x, (b) y, and (c) z coordinates.
(Keys: ——, CAPP-based ; ·····, geometry-based)

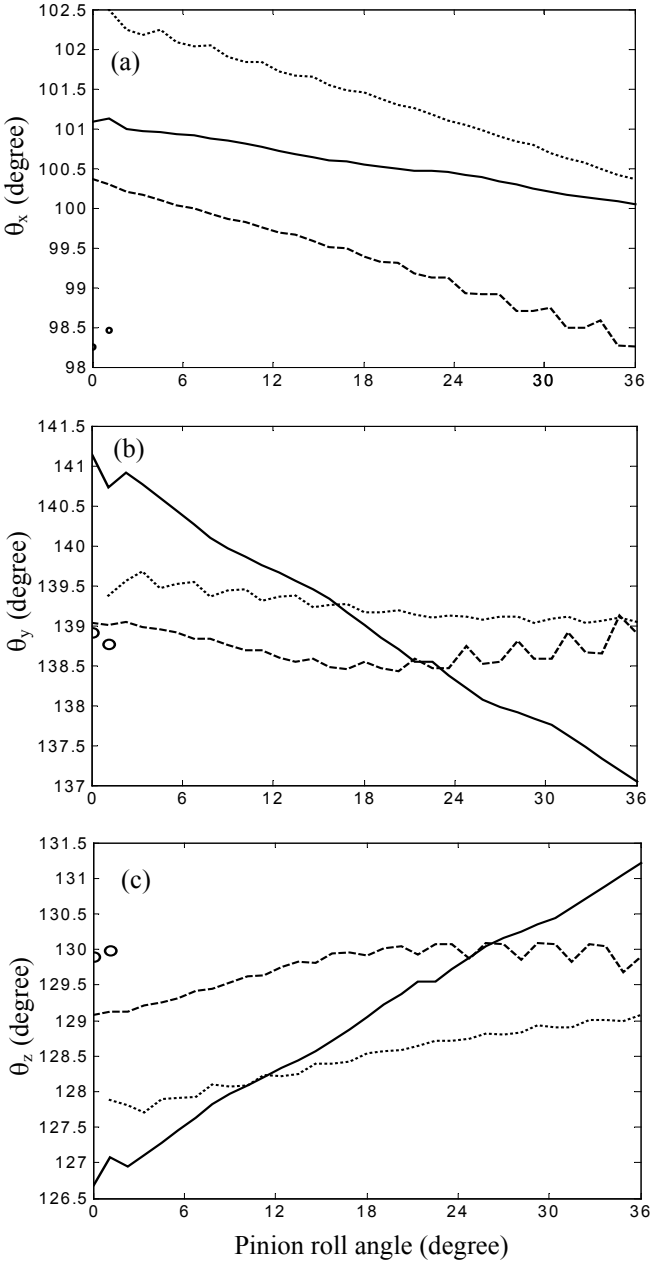

Figure 7. Effect of load on the directional cosine angles relative to the (a) x-axis, (b) y-axis, and (c) z-axis.
(Keys: ——, light load ; - - - -, tooth 1; ·····, tooth 2; o, tooth 3 under higher load)

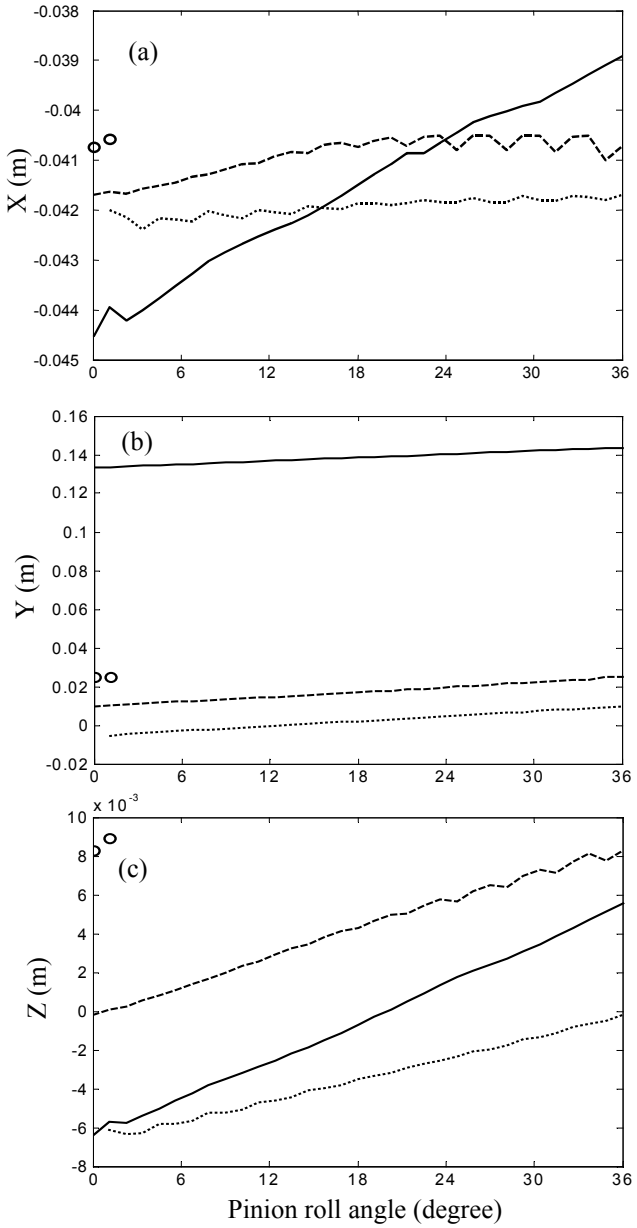

Figure 8. Effect of load on meshing point locations: (a) x, (b) y, and (c) z coordinates.
(Keys: ——, light load ; - - -, tooth 1; ·····, tooth 2; o, tooth 3 under higher load)

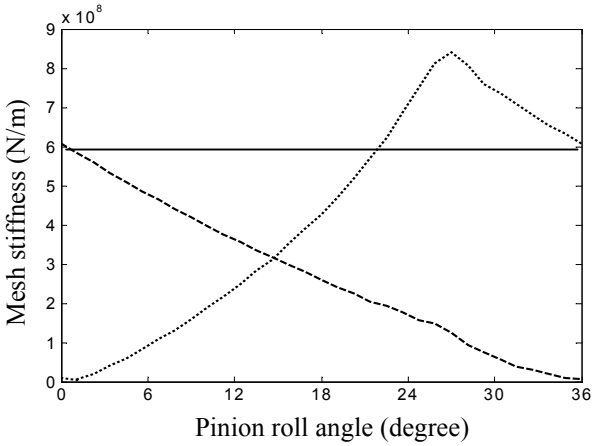

Figure 9. Mesh stiffness variation predicted from quasi-static tooth contact analysis.
(Keys: ——, time-invariant; - - -, tooth 1; ····· , tooth 2)

REFERENCES

[1] Kawasaki, K., and Tamura, H., 1998, "Duplex Spread Blade Method for Cutting Hypoid Gears with Modified Tooth Surface," *Journal of Mechanical Design*, **120**, pp. 441-447.

[2] Donno, M. D, and Litvin, F. L., 1999, "Computerized Design, Generation and Simulation of Meshing of a Spiroid Worm-gear Drive with a Ground Double-crowned Worm," *Journal of Mechanical Design*, **121**, pp. 264-273.

[3] Feng, P. H., and Litivn, F. L., 1999, "Determination of Principal Curvatures and Contact Ellipse for Profile Crowned Helical Gears," *Journal of Mech. Design*, **121**, pp. 107-121.

[4] Litivn, F. L., 1989, "Theory of Gearing", NASA RP-1212 (AVSCOM 88-C-035), Washington, D. C.

[5] Litivn, F. L., 1994, *Gear Geometry and Applied Theory*, Prentice-Hall, New York.

[6] Krenzer, T. J., 1981, "Tooth Contact Analysis of Spiral Bevel and Hypoid Gears under Load," SAE paper 810688.

[7] Gosselin, C., Cloutier, L., and Nguyen, Q. D., 1995, "A General Formulation for the Calculation of the Load Sharing and Transmission Error under Load of Spiral Bevel and Hypoid Gears," *Mech. Mach. Theory*, **30**, pp. 433-450.

[8] Mark, W. D., 1987, "The Generalized Transmission Error of Spiral Bevel Gears," *Journal of Mechanisms, Transmissions and Automation in Design*, **109**, pp. 275-282.

[9] Vijayakar, S., 1987, "Finite Element Methods for Quasi-prismatic Bodies with Application to Gears," *Ph.D Dissertation*, The Ohio State University, Columbus, Ohio.

[10] Kiyono, S., Fujii, Y., and Suzuki, Y., 1981, "Analysis of Vibration of Bevel Gears," *Bulletins of JSME*, **24**, pp. 441-446.

[11] Rautert, J., and Kollmann, F. G., 1989, "Computer Simulation of Dynamic Forces in Helical and Bevel Gears," Proc. 1989 Int. Power Transm. Gearing Conf.: New Technologies for Power Transmissions of the 90's, Chicago, IL, pp. 435-446.

[12] Donley, M. G., Lim, T. C., and Steyer, G. C., 1992, "Dynamic Analysis of Automotive Gearing Systems," *Journal of Passenger Cars*, **101**(6), pp. 77-87.

[13] Cheng, Y., and Lim, T. C., 1998, "Dynamic Analysis of High Speed Hypoid Gears with Emphasis on Automotive Axle Noise Problem," Proceedings, Power Transmission and Gearing Conf., ASME, Atlanta, Georgia, DETC98/PTG-5784.

[14] Lim, T. C., and Cheng, Y., 1999, "A Theoretical Study of the Effects of Pinion Offset on the Dynamics of Hypoid Geared Rotor System," *Journal of Mechanical Design*, **121**, pp. 1-8.

[15] Cheng, Y., and Lim, T. C., 2001, "Vibration Analysis of Hypoid Transmissions Applying an Exact Geometry-based Gear Mesh Theory," *Journal of Sound and Vibration*, **240**(3), pp. 519-543.

[16] Vijayakar, S., 1998, CAPP Users' Manual, Advanced Numerical Solutions, Hilliard, Ohio.